Geology

Quantifying postglacial sediment storage at the mountain-belt scale

Ralph K. Straumann and Oliver Korup

Geology 2009;37;1079-1082
doi: 10.1130/G30113A.1

Notes

Quantifying postglacial sediment storage at the mountain-belt scale

Ralph K. Straumann[1]* and Oliver Korup[2]
[1]Geographic Information Systems Division, Department of Geography, University of Zurich, CH-8057 Zurich, Switzerland
[2]Swiss Federal Research Institutes WSL/SLF, CH–7260 Davos, Switzerland

ABSTRACT

Sediment storage is an often-neglected term in sediment budgets, despite being the crucial link between rates of erosion and sediment yield. Mountain belts in particular host large valley fills that modulate fluxes of water and sediment, buffer the geomorphic coupling between hillslopes and river channels, reduce local valley relief, and protect bedrock from fluvial incision. Here we propose a region-growing algorithm based on a slope-gradient criterion to automatically extract areas of postglacial fluvial and lacustrine valley fills from digital topography at the mountain-belt scale. Applying this method to the European Alps, we find that the size-frequency relationship of 17,766 individual sediment storage units, expressed by either area or volume, follows a power law over four and five orders of magnitude with scaling exponents –1.77 and –1.71, respectively. We show that 90% of the area covered by sediment storage is in the lower quartile of the mountain belt's elevation and below the median local relief. On average, low-gradient valley fill occupies 6% of the studied drainage basins. This fraction increases with basin size, likely reflecting the larger accommodation space of trunk valleys generated by multiple glacial-interglacial cycles. Comparison with sediment storage mapped in the Southern Alps, New Zealand, indicates that rates of uplift and precipitation control the extent and spatial distribution of sediment storage at the mountain-belt scale.

INTRODUCTION

A number of studies have quantified the rates of erosion, sediment transport, and yield in mountain belts in historic or postglacial times (Church and Slaymaker, 1989; Hinderer, 2001). Comparatively few studies have tried to systematically quantify the distribution, volumes, or residence times of intermediate sediment storage such as floodplains, terraces, fans, moraines, and landslide debris that may occupy extensive tracts of mountain rivers (e.g., Wang et al., 2007). Yet sediment storage is a key term in the sediment budget, building a crucial link between erosion rate and sediment yield (Lu et al., 2005). At the mountain-belt scale, for example, volumetric estimates of dated molasse sediments allow inference of gross deposition and erosion over geological time scales (Kuhlemann et al., 2002). However, most studies that have attempted to quantify sediment storage in steep upland terrain focused on much smaller areas (Schrott et al., 2003; Kasai et al., 2004; Lancaster and Casebeer, 2007), and none are informative about the distribution and relevance of sediment storage at the mountain-belt scale.

This is a major shortcoming, especially as large intramontane valley fills modulate significantly fluxes of water and sediment, and help buffer the geomorphic coupling between hillslopes and river channels, thus delaying delivery of hillslope debris to the drainage network. On interglacial time scales large valley fills further contribute to reducing local valley relief, and protecting bedrock from erosion by fluvial incision and mass wasting (Sklar and Dietrich, 2001; Korup and Tweed, 2007). During glacial-interglacial cycles, the gradual replacement of glacial ice sheets by large bodies of postglacial sediment and vice versa affects glacio-isostatic and erosion-induced uplift (Champagnac et al., 2007). Deglaciation in particular may boost sediment yields through the rapid evacuation of large storage volumes (Koppes and Hallet, 2006).

In this regard, data on the spatial pattern and size distribution of sediment storage help set boundary conditions for numerical models of landscape evolution. Most of these models do not explicitly treat effects of large-scale sediment storage, which in formerly glaciated mountain belts should largely reflect the general downstream decrease in transport capacity, superimposed by effects of natural dams and glacially overdeepened bedrock basins (Korup and Tweed, 2007). Empirical evidence suggests that larger drainage basins can produce and store more postglacial sediment than smaller ones on average (e.g., Hinderer, 2001; Korup and Schlunegger, 2009). However, patterns of sediment storage at the mountain-belt scale have so far not been quantified.

Here we present a method for deriving, from a digital elevation model (DEM), valley-floor areas hosting extensive low-gradient sediment storage. Although numerous techniques have been proposed to objectively extract drainage networks from DEMs, there are few suggestions for delineating and quantifying areas of sediment storage (Williams et al., 2000; Gallant and Dowling, 2003; Noman et al., 2003; Demoulin et al., 2007). Our aim is to objectively quantify the distribution of sediment storage areas and volumes. We address this problem at the mountain-belt scale in order to integrate over a broad range of tectonic, climatic, and lithologic conditions, which influence the production, transport, and storage of sediment, and conclude by comparing effects of order-of-magnitude variations in these controls.

SETTING AND METHODS

Our study area occupies a large portion of the European Alps (Fig. 1). During the last glaciation, the Alps were covered by large ice streams that extended well beyond the mountain-range front, where large lakes attest to the terminal positions of valley glaciers. Few mountain peaks remained

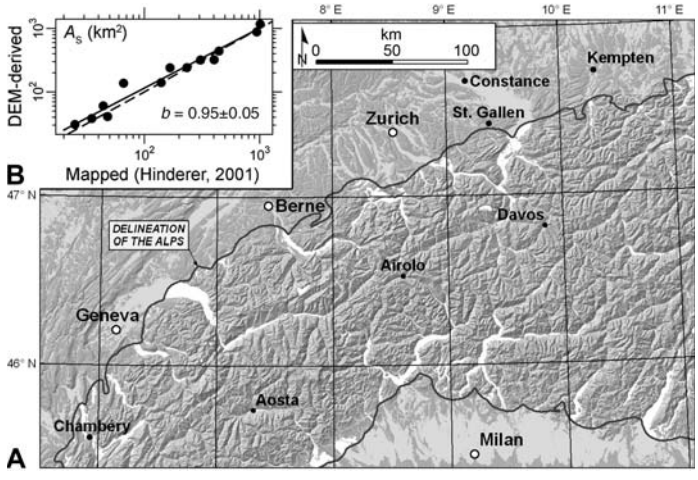

Figure 1. A: Study area in European Alps (delineated by dark gray line), and pattern of fluvial and lacustrine sediment storage (white), derived from 100 m digital elevation model (DEM) using region-growing algorithm with threshold of slope gradient of 1.5°. B: Sample comparison between DEM-derived and independently mapped areas of sediment storage (A_s) (Hinderer, 2001). Black line is reduced major axis with slope b = 0.95 ± 0.05 (±1σ), indicating near-linear relationship; dashed line is 1:1 ratio.

*E-mail: ralph.straumann@geo.uzh.ch.

ice free, while glaciers scoured valleys to bedrock. Therefore, all sediment accumulated in these valleys is assumed to be mainly of Late Glacial Maximum or younger age (Hinderer, 2001).

For the sake of our approach, we simplistically assume that individual areas of sediment storage A_S can be characterized as low-gradient terrain adjacent to the channel network. We used a hole-filled version of the Shuttle Radar Topography Mission DEM (SRTM V3; Jarvis et al., 2006) that we projected into Swiss National Grid coordinates and resampled to 100 m pixel resolution. For delineating the mountainous portion of the Alps we resampled the DEM to 1 km resolution, and computed local relief H as the maximum elevation range in a circular neighborhood of 15 km radius. Areas where $H > 1200$ m were arbitrarily classified as belonging to the Alps (Fig. 1A). In order to yield consistent results and a coherent study area, 6 small island polygons 1–35 km^2 in size were manually reassigned.

We filled sinks in the DEM and used the D8 single (steepest descent) flow direction and resulting flow accumulation to derive a Shreve-ordered drainage network with a channel initiation threshold of 5 km^2 for computational efficiency. Drainage basins of Shreve order X were then clipped by all drainage basins of order $Y < X$ to obtain what we term "drainage subbasins." A region-growing algorithm (RGA; Straumann and Purves, 2008) used the channel cells as seed cells and iteratively marked those cells as sediment storage area (A_S) that bordered the seed cells or previously marked A_S cells, and that fulfilled either of the following requirements:

$$\text{cardinal neighbors: } \tan(\gamma_c)\lambda \geq \Delta E \geq 0 \quad (1)$$

and

$$\text{diagonal neighbors: } \tan(\gamma_c)\lambda\sqrt{2} \geq \Delta E \geq 0, \quad (2)$$

where γ_c is an arbitrarily defined gradient threshold, λ is cell size, and ΔE is the elevation difference between the cell of interest and the adjacent seed or A_S cell. The RGA used $\gamma_c = 1.5°$, based on several trial-and-error runs that eventually returned the extent of large fluvial and lacustrine valley fills in a realistic manner, and was run iteratively until no new A_S cells were detected. The use of Shreve order segmented the drainage basins along the general flow direction, so that each river reach between two tributaries had its own drainage subbasin that confined uncontrolled overflow of A_S growth across subbasins. This procedure ensured that storage units were contiguous and that all low-gradient cells connected to the channel cells were classified as A_S. Thus delineated A_S cells were post-processed using expand and shrink procedures from mathematical morphology in order to generate individual patches of A_S instead of a single network feature of A_S connected through channel cells. This allowed quantifying A_S without the effect of channel cells.

SEDIMENT STORAGE IN THE ALPS

Our method produced $n = 17{,}766$ individual polygons of postglacial sediment storage that comprise fluvial valley fills and lakes, covering 5092 km^2 in total, i.e., 7% of our study area in the European Alps (65,940 km^2; Fig. 1). For a given drainage basin area, this first-order estimate compares well with valley fills independently mapped by Hinderer (2001; Fig. 1B). We do not expect a linear relationship, as the mapped areas of Hinderer (2001) also include large tributary fans, whereas the resolution of our approach may overestimate sediment storage in low-order basins. The size-frequency distribution of the DEM-derived sediment storage areas A_S has a power-law trend over four orders of magnitude with a scaling exponent $b_A = -1.77 \pm 0.03$ ($\pm 1\sigma$; Fig. 2). To estimate the volumes of individual sediment storage units, we computed the total area of storage in the basins shown in Figure 1B. We then used an empirical relationship between total postglacial sediment storage volume V_S estimated from borehole, seismic, and lake sedimentation data, and drainage basin area A_C (Hinderer, 2001) to obtain a power-law regression between V_S and A_S with exponent $\alpha = 1.12 \pm 0.15$ ($R^2 = 0.78$). The resulting density distribution of V_S has an exponent $b_V = -1.71 \pm 0.03$ (Fig. 2). In order to quantify the prediction error of this proposed volume-area scaling, we ran $n = 100$ Monte Carlo simulations, each using normally distributed exponent and intercept values for predicting the volume for each individual sediment storage unit. We consequently estimate the total volume of postglacial fluvial and lacustrine sediment storage at 411 ± 12 km^3 (±1 standard error) in the study area.

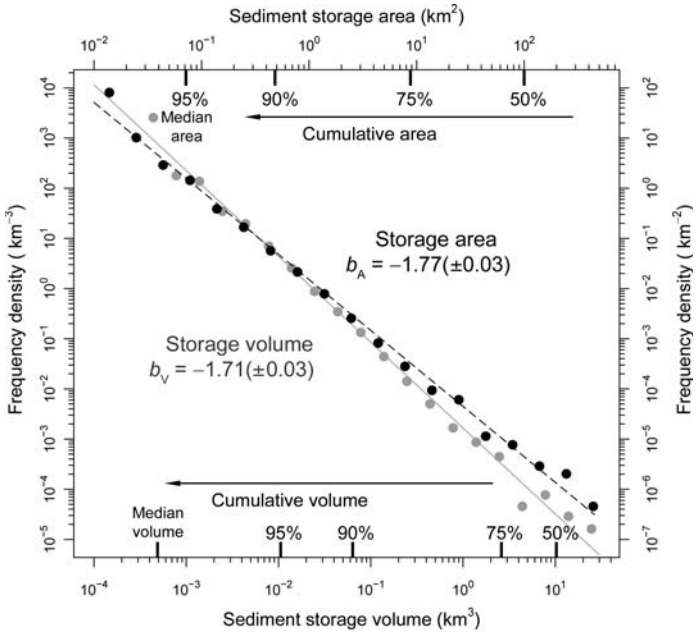

Figure 2. Noncumulative size-frequency relationships of fluvial and lacustrine valley fills in European Alps, based on n = 17,766 sediment storage units. Area and volume-density distributions have power-law trends over four and five orders of magnitude with estimated exponents b_A (black) and b_V (gray), respectively. Volume-density distribution was estimated from regression of total sediment storage volume (Hinderer, 2001) and A_S, with randomly iterated values of exponent $\alpha = 1.12 \pm 0.15$ ($\pm 1\sigma$) and intercept log $y = -1.52 \pm 0.35$. Interior ticks on x axes are cumulative fractions of total area and volume, and median values.

The total area covered by sediment storage is clearly dominated by the larger valley fills, and half of it is contained in the 11 largest (>100 km^2) fills, i.e., the broad Alpine valley floors feeding into the large glacially scoured lake basins at the mountain front (Fig. 1A). Correspondingly, large valley fills dominate the volumetric distribution of storage, with approximately half of all sediment being sequestered in the lower reaches of only nine trunk valleys (Fig. 2).

Hypsometric analysis confirms that ~90% of the total sediment storage area is below the 25th percentile of elevation (Fig. 3). Low-gradient fluvial and lacustrine sediment storage in the upper third of the mountain belt is negligible at the scale of this study. However, the question of whether to include river-channel cells with no adjacent A_S cells as actual storage elements in this estimate is not trivial. For example, the difference in normalized storage area ΔA made by including river-channel cells in the storage estimates is >5% between the 7th and 27th elevation percentile (Fig. 3). In other words, channel storage appears to have the highest contribution in the lower parts of the mountain belt. Moreover, 90% of the total sediment storage area is below the median local relief. This supports the view that most sediment is stored in areas of low erosion, assuming that local relief is a first-order proxy of postglacial erosion rates (e.g., Vance et al., 2003).

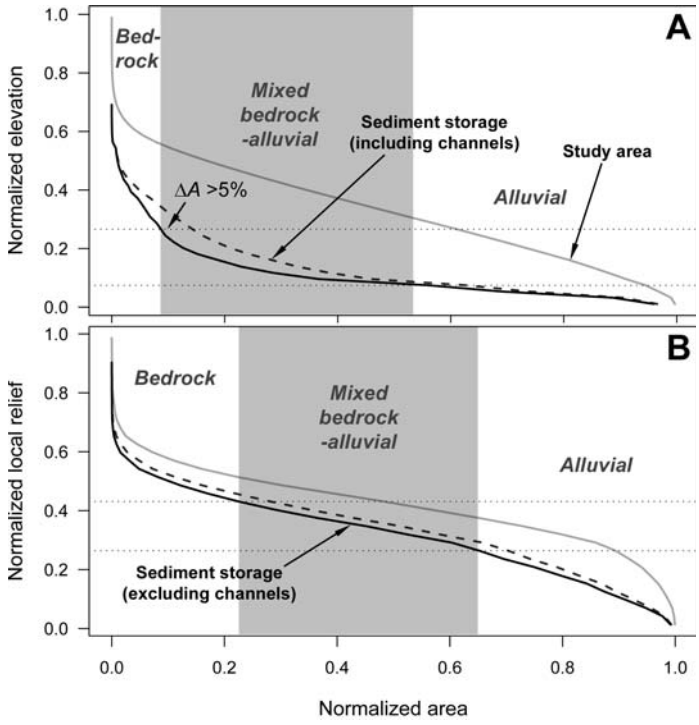

Figure 3. A: Hypsometry of study area (Fig. 1) and of sediment storage areas with and without channel cells. All curves are normalized to maximum elevation of 4700 m. Approximately 90% of the total sediment storage area (exclusive of river channels) is below 25th elevation percentile. Horizontal dotted lines bound elevation range where inclusion of channel cells as sediment storage leads to >5% difference in cumulative area ΔA, arbitrarily defining domain where mixed bedrock-alluvial rivers dominate (gray shaded). B: Hypsometry of local relief H (same symbols; normalized to maximum H = 3600 m).

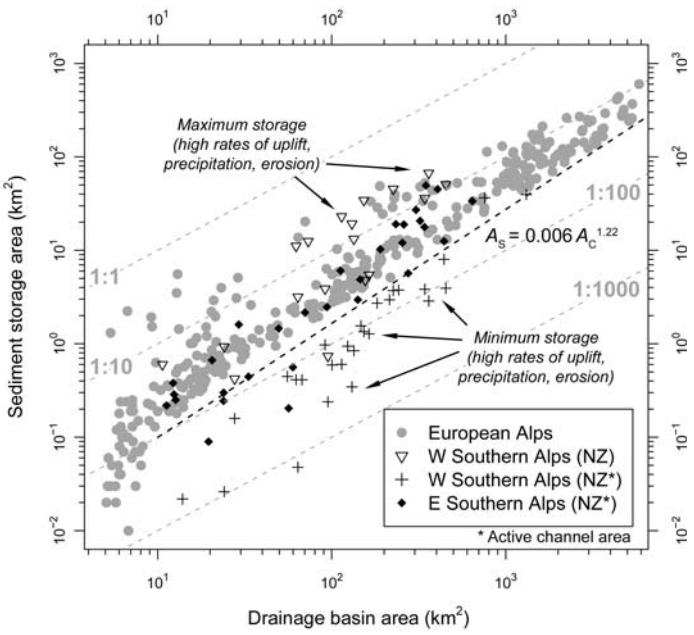

Figure 4. A: Random sample of n = 350 drainage basins (area, A_C >5 km²) and their digital elevation model (DEM)–derived areas of sediment storage A_S in European Alps; black dashed line is empirical lower envelope curve. Valley-fill data from Southern Alps, New Zealand (NZ), were mapped for comparison manually from 25 m DEM, and active channel areas (asterisk) obtained from 1:50,000 topographic maps. Gray dashed lines are ratios A_S/A_C.

In order to estimate the amount of sediment storage for a given point in the Alps, we assigned 50–100 random drainage basin outlets per order of magnitude of A_C. We find that the area of sediment storage units A_S above 350 such points increases nonlinearly with upstream basin area (Fig. 4). The fraction of sediment storage varies by three orders of magnitude in small headwater basins (A_C <10 km²), which are more prone to episodic sediment pulses and resulting aggradation, and less capable of buffering such disturbances. The channel initiation threshold of 5 km² used for generating the seed cells for the RGA may also be responsible for some of this scatter. On average, 5.8% (±4.5%) of basins >10 km² are covered by fluvial and lacustrine valley fill, and the minimum A_S increases by a factor of ~5 for 10 km² > A_C > 6000 km².

DISCUSSION AND CONCLUSIONS

We provide one of the first quantitative and solely DEM-derived estimates of postglacial fluvial and lacustrine sediment storage at the mountain-belt scale. Our results are first-order estimates and rest on several assumptions; nevertheless they agree well with earlier estimates without any prior calibration of sediment storage areas (Fig. 1B). Although the SRTM data are known to contain errors, especially in areas of high topographic roughness (Carabajal and Harding, 2005), the reliance of the RGA on relative elevation differences largely alleviates the effect of these errors. However, we suspect the method to have problems with too highly resolved data because of artifact noise and spurious slope gradients, especially in low-relief areas (Straumann and Purves, 2007).

Our results show that the mountain-belt scale pattern of postglacial sediment storage in the Alps is largely skewed. Larger valleys host by far the majority of postglacial debris (Fig. 2). We interpret this instance as a result of the creation of commensurately higher accommodation space through glacial overdeepening over the course of multiple glacial-interglacial cycles. The importance of river channels as potential storage units is highest in lower levels of the mountain belt (Fig. 3). Moreover, considering the effect of channel storage allows quantifying objectively the downstream transition between three fundamental process domains of the fluvial system, i.e., bedrock rivers, alluvial rivers, and mixed bedrock-alluvial rivers, at the mountain-belt scale. Although the distinction between these domains depends on an arbitrarily defined threshold value of added contribution of channel storage ΔA (i.e., 5% in the case of Fig. 3), our data indicate that bedrock rivers appear to dominate upper-level and high-relief portions of the Alps. This notion awaits further testing with field evidence, but the essence of our method as a potential predictor of river types remains regardless of the eventual choice of ΔA.

Comparing our results with valley-fill data from the Southern Alps, New Zealand, allows exploring the effects on sediment storage of higher variance in rates of uplift, precipitation, and rock type (Fig. 4). Active channel areas in the eastern Southern Alps were obtained from 1:50,000 topographic maps, and chiefly represent broad, extensive valley trains featuring braided rivers that entail most of the valley width, thus closely approximating A_S. We assume that rates of rock uplift (U ~1–2 mm yr⁻¹) and precipitation (P <2000 mm yr⁻¹) in the eastern Southern Alps are comparable to those in the European Alps at the regional scale (Fitzsimons and Veit, 2001). Active channel areas in the western Southern Alps, where U and P are one order of magnitude higher than in the eastern Southern Alps, are smaller, more patchy, limited to local alluviation of otherwise steep bedrock-dominated rivers, and constitute <5% of a given drainage basin area (Fig. 4). Yet most of the larger rivers are backfilled by large alluvial fans at the mountain range front (Davies and Korup, 2007). Thus, we also mapped manually the full extent of valley fills in the western Southern

Alps, including floodplains, terraces, lakes, alluvial fans, moraines, and debris fans, from geological maps and a 25 m DEM.

Overall, the New Zealand data extend the range of tectonic and climatic forcing conditions and provide a wider context for the pattern of sediment storage in the Alps. The western Southern Alps data help sketch tentative upper and lower envelope curves to sediment storage in steep topography dominated by high rates of rock uplift, precipitation, and erosion (Fig. 4). The match of active channel areas in the eastern Southern Alps and the Alps over nearly two orders of drainage basin size is particularly striking. We surmise that this indicates that formerly glaciated mountainous topography at comparable levels of tectonic and climatic forcing may accumulate similar fractions of postglacial sediment storage for a given drainage basin size, regardless of differences in rock type or land cover.

ACKNOWLEDGMENTS

This work was partly funded by European Commission Contract 045335 TRIPOD. We thank Ross Purves and three anonymous reviewers for encouraging comments.

REFERENCES CITED

Carabajal, C.C., and Harding, D.J., 2005, ICESat validation of SRTM C-band digital elevation models: Geophysical Research Letters, v. 32, L22S01, doi: 10.1029/2005GL023957.

Champagnac, J.D., Molnar, P., Anderson, R.S., Sue, C., and Delacou, B., 2007, Quaternary erosion-induced isostatic rebound in the western Alps: Geology, v. 35, p. 195–198, doi: 10.1130/G23053A.1.

Church, M., and Slaymaker, O., 1989, Disequilibrium of Holocene sediment yield in glaciated British Columbia: Nature, v. 337, p. 452–454, doi: 10.1038/337452a0.

Davies, T.R.H., and Korup, O., 2007, Persistent alluvial fanhead trenching resulting from large, infrequent sediment inputs: Earth Surface Processes and Landforms, v. 32, p. 725–742, doi: 10.1002/esp.1410.

Demoulin, A., Bovy, B., Rixhon, G., and Cornet, Y., 2007, An automated method to extract fluvial terraces from digital elevation models: The Vesdre valley, a case study in eastern Belgium: Geomorphology, v. 91, p. 51–64, doi: 10.1016/j.geomorph.2007.01.020.

Fitzsimons, S.J., and Veit, H., 2001, Geology and geomorphology of the European Alps and the Southern Alps of New Zealand: A comparison: Mountain Research and Development, v. 21, p. 340–349, doi: 10.1659/0276-4741(2001)021[0340:GAGOTE]2.0.CO;2.

Gallant, J.C., and Dowling, T.I., 2003, A multiresolution index of valley bottom flatness for mapping depositional areas: Water Resources Research, v. 39, 1347, doi: 10.1029/2002WR001426.

Hinderer, M., 2001, Late Quaternary denudation of the Alps, valley and lake fillings and modern river loads: Geodinamica Acta, v. 14, p. 231–263, doi: 10.1016/S0985-3111(01)01070-1.

Jarvis, A., Reuter, H.I., Nelson, A., and Guevara, E., 2006, Hole-filled seamless SRTM data V3: International Centre for Tropical Agriculture (CIAT), http://srtm.csi.cgiar.org.

Kasai, M., Marutani, T., and Brierley, G.J., 2004, Patterns of sediment slug translation and dispersion following typhoon-induced disturbance, Oyabu Creek, Kyushu, Japan: Earth Surface Processes and Landforms, v. 29, p. 59–76, doi: 10.1002/esp.1013.

Koppes, M., and Hallet, B., 2006, Erosion rates during deglaciation in Icy Bay, Alaska: Journal of Geophysical Research, v. 111, F02023, doi: 10.1029/2005JF000349.

Korup, O., and Schlunegger, F., 2009, Rock type control on erosion-induced uplift in the eastern Swiss Alps: Earth and Planetary Science Letters, v. 278, p. 278–285, doi: 10.1016/j.epsl.2008.12.012.

Korup, O., and Tweed, F., 2007, Ice, moraine, and landslide dams in mountainous terrain: Quaternary Science Reviews, v. 26, p. 3406–3422, doi: 10.1016/j.quascirev.2007.10.012.

Kuhlemann, J., Frisch, W., Székely, B., Dunkl, I., and Kázmér, M., 2002, Post-collisional sediment budget history of the Alps: Tectonic versus climatic control: International Journal of Earth Sciences, v. 91, p. 818–837, doi: 10.1007/s00531-002-0266-y.

Lancaster, S.T., and Casebeer, N.E., 2007, Sediment storage and evacuation in headwater valleys at the transition between debris-flow and fluvial processes: Geology, v. 35, p. 1027–1030, doi: 10.1130/G239365A.1.

Lu, H., Moran, C.J., and Sivapalan, M., 2005, A theoretical exploration of catchment-scale sediment delivery: Water Resources Research, v. 41, W09415, p. 2005, doi: 10.1029/2004WR003037.

Noman, N.S., Nelson, E.J., and Zundel, A.K., 2003, Improved process for floodplain delineation from digital terrain models: Journal of Water Resources Planning and Management, v. 129, p. 427–436, doi: 10.1061/(ASCE)0733-9496(2003)129:5(427).

Schrott, L., Hufschmidt, G., Hankammer, M., Hofmann, T., and Dikau, R., 2003, Spatial distribution of sediment storage types and quantification of valley fill deposits in an alpine basin, Reintal, Bavarian Alps, Germany: Geomorphology, v. 55, p. 45–63, doi: 10.1016/S0169-555X(03)00131-4.

Sklar, L.S., and Dietrich, W.E., 2001, Sediment and rock strength controls on river incision into bedrock: Geology, v. 29, p. 1087–1090, doi: 10.1130/0091-7613(2001)029<1087:SARSCO>2.0.CO;2.

Straumann, R.K., and Purves, R.S., 2007, Resolution sensitivity of a compound terrain derivative as computed from LiDAR-based elevation data, *in* Fabrikant, S.I., and Wachowicz, M., eds., The European Information Society: Leading the way with geo-information: Lecture Notes in Geoinformation and Cartography, Proceedings of the 2007 AGILE International Conference, v. 18: Berlin, Springer, p. 87–109.

Straumann, R.K., and Purves, R.S., 2008, Delineation of valleys and valley floors, *in* Cova, T.J., et al., eds., Proceedings of the 5th international conference on Geographic Information Science: Lecture Notes In Computer Science, v. 5266: Berlin, Springer, p. 320–336.

Vance, D., Bickle, M., Ivy-Ochs, S., and Kubik, P.W., 2003, Erosion and exhumation in the Himalaya from cosmogenic isotope inventories of river sediments: Earth and Planetary Science Letters, v. 206, p. 273–288, doi: 10.1016/S0012-821X(02)01102-0.

Wang, Z.Y., Li, Y., and He, Y., 2007, Sediment budget of the Yangtze River: Water Resources Research, v. 43, W04401, doi: 10.1029/2006WR005012.

Williams, W.A., Jensen, M.E., Winne, J.C., Redmond, and R.L., 2000, An automated technique for delineating and characterizing valley-bottom settings: Environmental Monitoring and Assessment, v. 64, p. 105–114.

Manuscript received 6 February 2009
Revised manuscript received 9 July 2009
Manuscript accepted 11 July 2009

Printed in USA